Preparation and Properties of Polysulfone–Clay Composite Membranes

Orietta Monticelli, Aldo Bottino, Ivan Scandale, Gustavo Capannelli, Saverio Russo

Dipartimento di Chimica e Chimica Industriale, Università di Genova and Interuniversity Consortium on Materials Science and Technology Multifunctional Polymeric Nanocomposites and Hybrids Laboratory Centre, Via Dodecaneso 31, 16146 Genova, Italy

Received 18 January 2006; accepted 8 May 2006
DOI 10.1002/app.25511
Published online in Wiley InterScience (www.interscience.wiley.com).

ABSTRACT: Porous membranes and dense films were prepared from polysulfone solutions in *N*-methyl-2-pyrrolidone (NMP) containing different types and amounts of clay. Commercial clays supplied by Southern Clay, either unmodified (Cloisite Na) or organically modified (Cloisite 30B and Cloisite 93A), were used. The clay behavior in the organic solvent was dependent on the presence and type of the organic compatibilizer: Cloisite containing Na ions did not swell in NMP, whereas those with the organic compatibilizer swelled, though to a different degree. Electron microscopy observations were made to examine the clay dispersion in the membrane structure. At variance with Cloisite Na and Cloisite 93A formed microaggregates, Cloisite 30B yielded nanostructures composed of both single sheets and well-ordered multilayer silicate clusters, which were characterized by an interlayer distance higher than that of the neat clay. The increase in the distance between the layers of Cloisite 30B was related to the formation of intercalated nanocomposites, whereas the presence of single sheets well distributed in the polymer matrix supported the occurrence of delaminated nanocomposites. The intercalation of the polymer into clay layers was confirmed with wide-angle X-ray diffractometry. The addition of Cloisite 30B to the casting solution influenced the phase-separation process in the coagulation bath. Therefore, by the variation of the layered-silicate concentration in the casting solution, membranes with different morphological structures and ultrafiltration properties were obtained. Cloisite 30B was also found to improve the wettability and mechanical properties of dense films. J Appl Polym Sci 103: 3637–3644, 2007

Key words: membranes; nanocomposites; polysulfone

INTRODUCTION

Composite membranes and films based on polymeric matrices and inorganic fillers have attracted great interest in recent years for their peculiar features. Compared with the neat polymers, these novel organic–inorganic materials, exploited in the field of membranes, can potentially enhance the operating temperature and pressure, improve the chemical stability, increase the selectivity and permeability, and finally reduce the fouling tendency.

So far, studies have mainly focused on a wide range of membrane separation processes, such as gas separation,[1] pervaporation,[2] nanofiltration, and ultrafiltration.[3,4]

Among the various inorganic fillers (zeolites,[2,5] inorganic and ceramic oxides,[4,6–8] etc.) used to prepare composite membranes and films, layered silicalites deserve special attention because of their ability to be dispersed in the polymeric matrices at a nanoscopic level. The commonly used layered silicates for the preparation of these nanocomposites belong to the family of 2 : 1 layered silicates or phyllosilicates. The crystal structure of the materials consists of layers made up of two tetrahedrally coordinated silicon atoms fused to an edge-shared octahedral sheet of either aluminum or magnesium hydroxide.

In general, polymer/layered-silicalite nanocomposites exhibit improvements in material properties, such as higher moduli, increased strength and heat resistance, decreased flammability, and increased biodegradability for biodegradable polymers.[9] Films based on phyllosilicates, dispersed to form intercalated or exfoliated nanocomposites, show gas-barrier properties.[10–13] The large reduction of the permeability coefficient has been explained by an increase in the total pathway of the gas along the film.[13]

Recently, interesting applications of nanocomposite membranes containing phyllosilicates have been reported in the field of fuel cells. Nafion/montmorillonite (MMT) nanocomposite membranes were applied to direct methanol fuel cells.[14] The membranes were obtained by the direct melt intercalation of perfluorosulfonylfluoride copolymer resin (Nafion) into either MMT or organically modified MMT. The performance of the membrane–electrode assembly was higher than that of a Nafion commercial membrane operating at a high temperature.

Correspondence to: O. Monticelli (orietta@chimica.unige.it).
Contract grant sponsor: Ministero dell'Istruzione dell'Università e della Ricerca (through the FIRB 2001 project MAPIONANO).

Alberti et al.[15] reported the use of layered zirconium sulfoarylphosphonates to prepare composite membranes with high proton conductivity and good stability at medium temperatures.

Despite the potential properties of these nanocomposite membranes in the field of ultrafiltration or nanofiltration, only a few studies have been conducted to develop this aspect. Cheng et al.[16] prepared a novel microporous membrane from mica-intercalated nylon 6 by a phase-inversion method. The structure of the nanocomposite membrane turned out to be completely different from that prepared from a solution containing only the polyamide.

In this work, we report on the preparation of nanocomposite membranes based on polysulfone (PSU) and commercial MMT with the phase-inversion method. The polymer intercalation into the phyllosilicate structure was performed from solutions containing the solubilized polymer and the swollen clays. The clay dispersion in the polymeric matrix was evaluated by means of transmission electron microscopy (TEM) and X-ray diffraction measurements. To study the influence of the phyllosilicate on the mechanism of membrane formation, cloud-point measurements were carried out. Membrane properties were evaluated in terms of the water flux, dextran retention, and tensile strength. Moreover, an appraisal of the membrane hydrophilicity was obtained from contact-angle measurements for the corresponding dense films.

EXPERIMENTAL

Materials

PSU was a commercial product (Milan, Italy) (UDEL P-3500, Solvay). *N*-Methyl-2-pyrrolidone (NMP; >99%; Aldrich, Milan, Italy) was used as a polymer solvent. The structure of the monomeric unit is shown in Figure 1. Details on the typical physical properties of the polymer are available on the website (www.solvayadvancedpolymers. com) of the manufacturer.

The sodium and organically modified MMTs (under the commercial name of Cloisite) were supplied by Southern Clay (Gonzales, TX). Two organophilic clays, Cloisite 30B and Cloisite 93A, were used. The latter was modified by methyl dehydrogenated tallow ammonium salt, whereas Cloisite 30B contained a methyl tallow bis-2-hydroxyethyl quaternary ammonium salt as an organic compatibilizer.

Membrane and film preparation

Binary solutions were prepared by the dissolution of PSU (25 wt %) in NMP at room temperature. Ternary dispersions were obtained by the addition of different amounts of clay (from 2 to 5 wt %) to 100 g of a binary solution.

The solution and dispersion were first cast onto a glass plate with a proper knife to form a thin film (ca. 350 μm thick) that, in the case of membrane preparation, after a 30-s exposure period in a controlled environment (air at 20°C and 60% relative humidity), were immersed in water at 20°C to induce precipitation of the polymer and porous membrane formation. After a 5-min immersion period, the membranes were detached from the plate and leached overnight under running water before characterization.

Dense (nonporous) films were obtained by the evaporation of NMP from the cast solution through overnight exposure in an oven at 110°C.

Cloud-point measurements were carried out by the titration of the polymer solutions with a concentration of 20 wt % PSU in NMP, to which 2, 3, or 5 wt % Cloisite 30B was added. The cloud point is defined as the composition at which the solution did not become clear again after 12 h of homogenization.

Membrane and film characterization

A Leica Stereoscan 440 scanning electron microscope (Wetzlar, Germany) was used to examine the membrane structure and clay dispersion. All specimens were coated with a thin layer of gold before scanning electron microscopy (SEM) observations. TEM and wide-angle X-ray diffraction (WAXD) were used to evaluate the presence of nanostructures. WAXD patterns were recorded with a Philips PW 1830 powder diffractometer (Amelon, The Netherlands) (Ni-filtered Cu Kα radiation). TEM measurements were performed with a JEOL 2010 high-resolution instrument (Tokyo, Japan). Ultrathin sections about 100 nm thick were cut with a Power Tome X microtome (Tucson, AZ) equipped with a diamond knife and placed on a 200-mesh copper grid.

Ultrafiltration tests were carried out with a laboratory-scale unit, described elsewhere,[17] which was fed

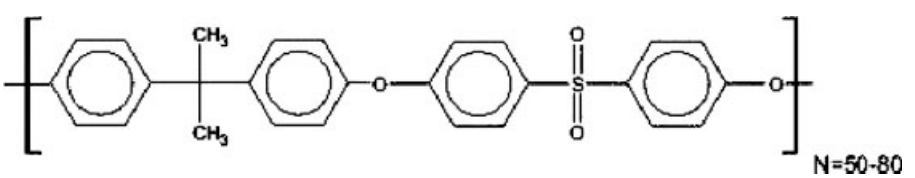

Figure 1 Monomeric unit structure of UDEL P-3500.

with a 100 ppm aqueous solution of dextran (nominal average molecular mass = 40 kDa). The dextran solution flowed tangentially to the membrane surface (66×10^{-4} m^2) under the following operating conditions: a pressure of 2 bar, a temperature of 25°C, and a flow rate of 5 m/s. The dextran concentration was kept constant by the recirculation of both the permeate and retentate to the feed tank of the unit. No variation in the membrane performance (permeate flux and retention) was observed during the entire duration (120 min) of the ultrafiltration test.

The permeate flux [F (L/m^2 h)] was determined as follows:

$$F = Q/A$$

where Q (L/h) and A (m^2) represent the permeate flow rate and the membrane surface, respectively.

The retention (R) was calculated as follows:

$$R(\%) = (D_C - D_P)/D_C \times 100 \quad (1)$$

where D_C and D_P represent the dextran concentrations in the retentate and permeate, respectively.

Both concentrations were determined colorimetrically.[18]

The contact-angle measurements were performed at room temperature with an Erma G-1 contact angle meter (Tokyo, Japan) with pure water as the probe liquid.

The film mechanical properties were measured with an Instron model 5500 dynamometer (Milan, Italy). The elastic modulus, strength, and strain at break were calculated from the stress–strain curves as the average of at least 15 measurements.

RESULTS AND DISCUSSION

As mentioned previously, neat and composite membranes based on PSU were prepared with NMP as the casting solvent. The choice of the solvent was mainly due to the good solubility of the polymer matrix in it. In this respect, it is relevant to underline that the selection of a suitable solvent, capable not only of completely solubilizing the polymer but also finely dispersing the clay, is essential for good polymer intercalation into silicate galleries. Indeed, the role of the solvent in nanocomposite formation was studied by Shen et al.,[19] who found that poly(ethylene oxide) does not intercalate well into organically modified bentonite from toluene, but it does from chloroform.

In our case, the clay behavior in the organic solvent was found to be dependent on the presence and type of the organic compatibilizer: Cloisite containing Na ions did not swell in NMP and formed coarse dispersions, whereas those with the organic compatibilizer swelled, though to a different degree [the swelling factor (S) for Cloisite 30 is 50, whereas that for Cloisite 93A is 25). S can be defined with the following equation: $S = (V_s - V_c)/V_c$, where V_c represents the volume of the dry powder and V_s is defined as the volume of the slurry, that is, the sedimented volume of the swollen nanoclay in NMP measured after 24 h at room temperature. Although this parameter is not related to the layered-silicate swelling at a real nano-

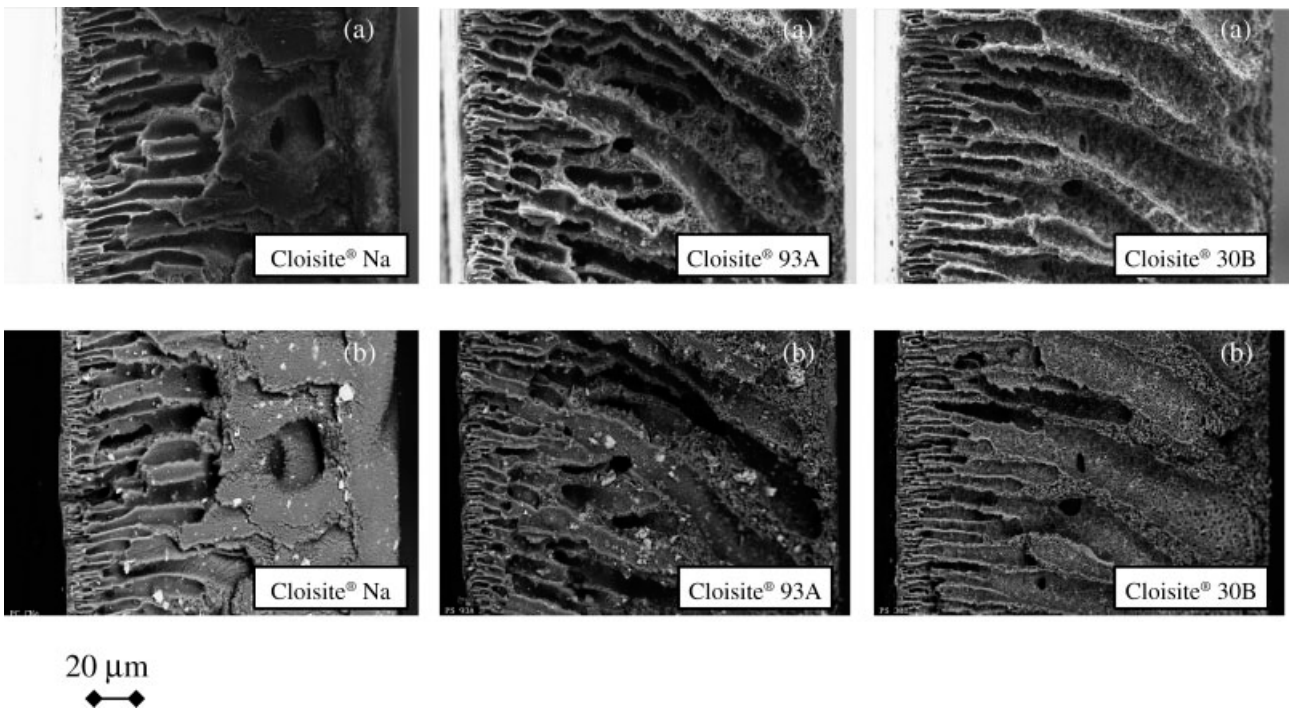

Figure 2 SEM micrographs of PSU/Cloisite Na, PSU/Cloisite 93A, and PSU/Cloisite 30B membrane cross sections (clay concentration = 2 wt %): (a) secondary-electron emission and (b) backscattering emission.

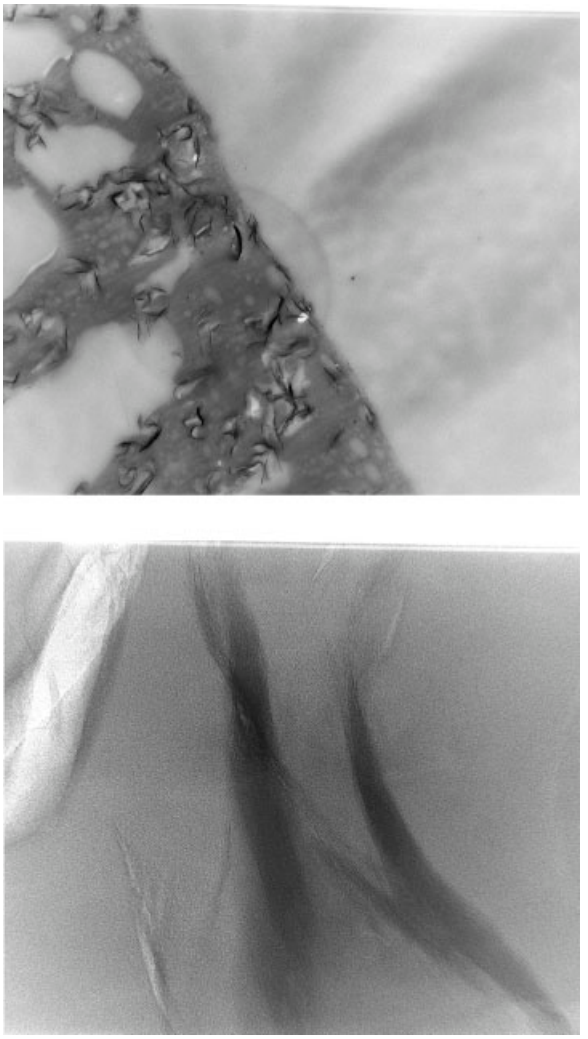

Figure 3 TEM micrographs of a PSU/Cloisite 30B membrane (clay concentration = 2 wt %).

scopic level, it can give an idea about solvent/clay interactions.[20]

Also, the results of a preliminary investigation (not reported in this article) on the rheological properties of the binary solutions and ternary dispersions seems to indicate a connection between the higher viscosities observed for the ternary NMP–PSU–organoclay systems with respect to the PSU–NMP binary solutions and the solvent/clay interactions.

PSU/Cloisite membrane morphology

Both membrane cross sections and surfaces were examined in detail by SEM. Figure 2 compares the micrographs of membrane cross sections obtained by secondary-electron emission and those by backscattering emission.

The backscattering electron emission allowed us to identify the presence and distribution of Si in the polymer matrix and hence to study the layered-silicate dispersion in the membranes.

An analysis of the photographs shows that the Si dispersion depends on the type of clay used. A homogeneous dispersion of Cloisite Na and 93A aggregates can be clearly observed. This finding highlights the occurrence of such composite membranes, whose formation is likely to follow the mechanism of other types of composite membranes based on different inorganic fillers.[21,22] Conversely, no aggregates are present in the composite membrane prepared from Cloisite 30B.

A deeper insight into Si dispersion has been provided by TEM measurements (Fig. 3), which provide evidence of the clay dispersion in the membrane cross section.

An inspection of TEM micrographs taken at a higher magnification reveals the presence of both single sheets and well-ordered multilayer silicate clusters, which have an interlayer distance of about 2.5–3 nm. The increase in the distance among the layers of Cloisite 30B (neat Cloisite 30B exhibits an interlayer distance of 1.8 nm) is related to the formation of intercalated nanocomposites, whereas the presence of single sheets, distributed in the polymer matrix, shows the occurrence of delaminated nanocomposites.

To confirm polymer intercalation into the phyllosilicate layers, the increase in the (001) *d*-spacing was measured by X-ray diffraction on dense films, which were prepared from the same casting solutions used for the membrane preparation.

Table I shows the interlayer distances of the neat clays and composite films. As expected, the (001) *d*-spacing of Cloisite 93A and Cloisite Na only changes slightly in the films, indicating irrelevant polymer intercalation inside the phyllosilicate layers. On the contrary, PSU seems to be well intercalated in Cloisite 30B. The latter finding is, indeed, proof of the possibility of preparing nanocomposite membranes based on PSU and commercial clays.

As previously mentioned, one of the few examples dealing with the preparation of a nanocomposite porous membrane with a phyllosilicate (i.e., mica) was reported by Cheng et al.[16] In that work, a novel microporous membrane was synthesized from mica-interca-

TABLE I
Interlayer Distances of the Clay Powders and Composite Films

Clay type	Film type	Clay concentration (wt %)	Interlayer distance (nm)
Cloisite Na	—	—	1.17
Cloisite 30B	—	—	1.74
Cloisite 93A	—	—	2.60
Cloisite Na	PSU/Cloisite Na	2	1.30
Cloisite 30B	PSU/Cloisite 30B	2	2.50
Cloisite 93A	PSU/Cloisite 93A	2	2.91

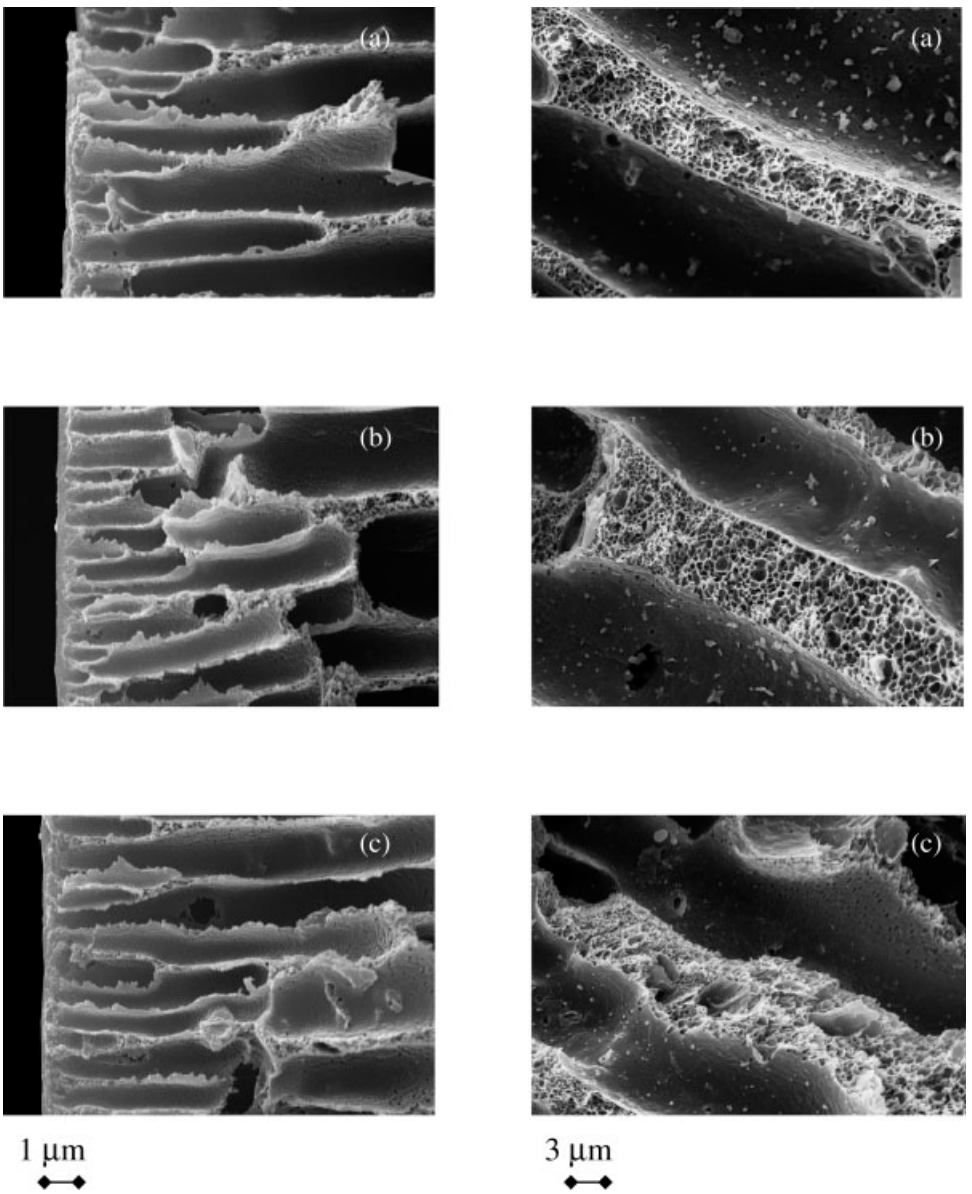

Figure 4 SEM micrographs of PSU/Cloisite Na membranes: (a) 2, (b) 3, and (c) 5 wt % clay.

lated nylon 6 by a phase-inversion process. The novel membrane turned out to be skinless and composed of cellular pores and sheaflike crystallites.

Our approach is different, as intercalation of the organically modified phyllosilicate occurs directly and more simply in the polymer solution. The basic advantage of our technique lies in the possibility of preparing nanocomposite membranes by simple immersion in a nonsolvent bath.

Figures 4 and 5 show SEM micrographs of cross sections of membranes based on Cloisite Na and Cloisite 30B, respectively. The membranes were prepared by the addition of different amounts of clay to PSU solutions (from 2 to 5 wt %).

Two different areas of the cross section were examined at a higher magnification to better evaluate the changes induced by clay addition. As far as the Cloisite 30B membrane is concerned, it seems that with an increase in the Cloisite concentration, the skin-layer thickness shows a tendency to decrease, whereas the porosity of the walls between the finger-like cavities increases. On the contrary, in Cloisite Na membranes, an opposite trend, similar to that found for traditional composite organic/inorganic membranes, can be observed.

To further investigate the influence of clay on membrane formation, cloud-point measurements were carried out. Obviously, only transparent starting systems made of NMP, PSU, and Cloisite 30B were considered for cloud-point tests.

Table II shows that the water content at the cloud-point increases as the Cloisite concentration increases in the casting solution. Indeed, the higher water tolerance as well as the increase in the viscosity caused by

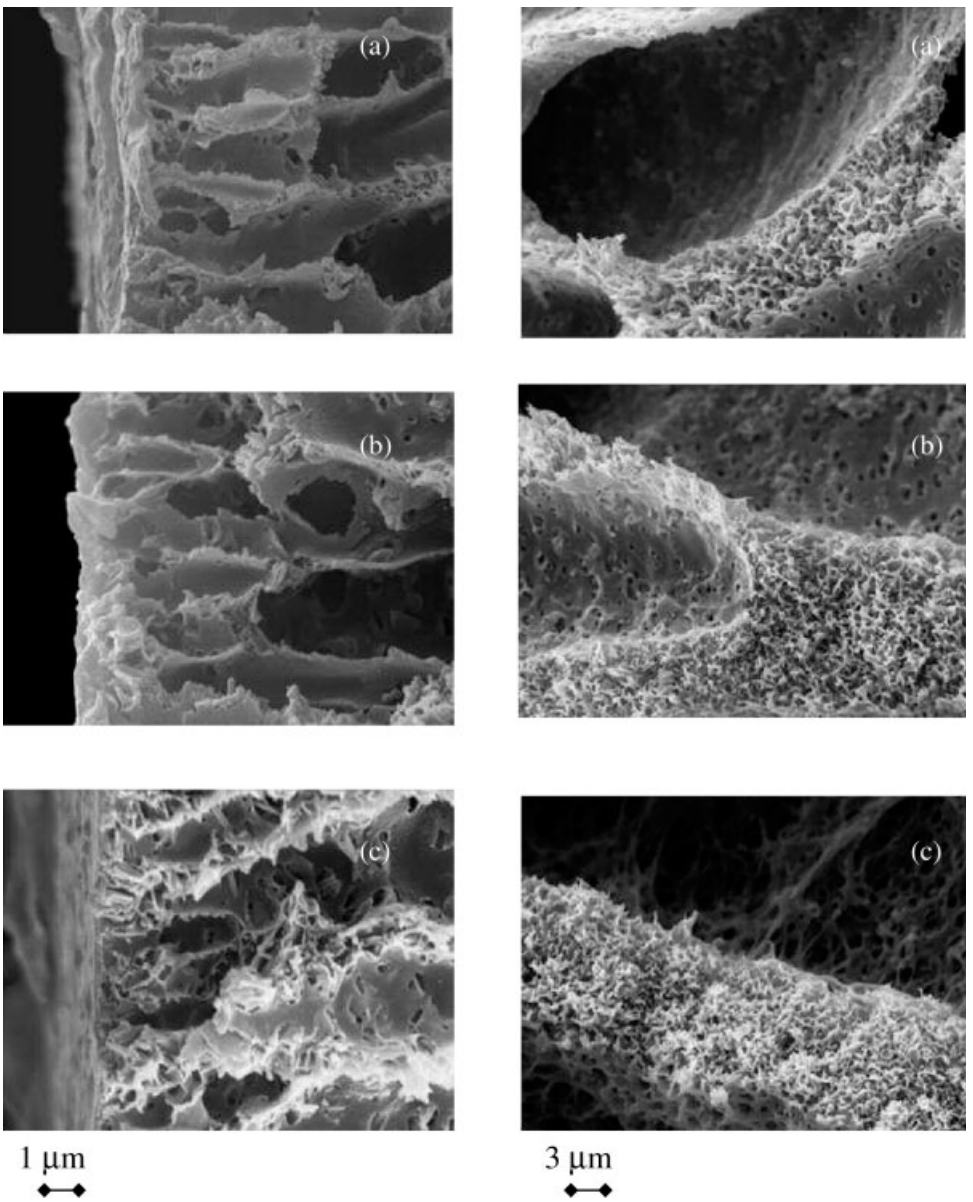

Figure 5 SEM micrographs of PSU/Cloisite 30B membranes: (a) 2, (b) 3, and (c) 5 wt % clay.

clay addition to the PSU solution may affect the mechanism of membrane formation in the water coagulation bath and, consequently, the characteristics of both the membrane skin layer and those of the fingerlike cavities beneath the skin, as depicted in Figure 5.

TABLE II
Clouds Points of the PSU/Cloisite 30B® Solution

Solution type	Clay concentration (wt %)	Water content at cloud point ($gH_2O/gPSU$)
PSU	—	2.52
PSU/Cloisite 30B®	2	3.12
PSU/Cloisite 30B®	3	4.63
PSU/Cloisite 30B®	5	4.56

PSU concentration, 20 wt %; NMP concentration, 80 wt %.

Because water addition seems not to favor Cloisite agglomeration, clay layers, as formed in the casting solution, remain well separated during immersion in the coagulation bath by the precipitated polymer, and consequently, a nanocomposite membrane is obtained.

TABLE III
Flux (*F*) and Dextran Retention (*R*) of the Membranes

Membrane	Clay concentration (wt %)	F ($L\ m^{-2}\ h^{-1}$)	R (%)
PSU	—	0.58	2.0
PSU/Cloisite 30B	2	192.02	20.6
PSU/Cloisite 30B	5	226.71	0
PSU/Cloisite Na	2	1.07	92.2
PSU/Cloisite Na	5	0.49	76.7
PSU/Cloisite 93A	2	14.84	86.6

TABLE IV
Contact Angles of Films Characterized by Different Clay Concentrations

Film type	Clay concentration (wt %)	Contact angle (°)
PSU	—	80
PSU/Cloisite Na	1	79
PSU/Cloisite Na	2	80
PSU/Cloisite Na	3	78
PSU/Cloisite Na	5	80
PSU/Cloisite 30B	2	70
PSU/Cloisite 30B	3	61
PSU/Cloisite 30B	5	64
PSU/Cloisite 93A	2	79

PSU/Cloisite membrane properties

From the results of the ultrafiltration tests listed in Table III, it appears that both the water flux and dextran retention are strongly influenced by the type of clay and its concentration.

These results seem to be in excellent agreement with the findings based on microscopic observations. Cloisite 30B yields membranes that are very porous, holding the highest flux and the lowest retention. That is, the water permeability increases with increasing layered-silicate content, whereas the retention decreases and reaches the zero value for the membrane containing 5 wt % clay. Nevertheless, the membrane with a low Cloisite concentration (2 wt %) turns out to have interesting characteristics for ultrafiltration applications (i.e., high flux and acceptable retention).

On the contrary, membranes prepared from Cloisite Na show good retention but very low flux. The performances of these membranes do not appear very useful for practical applications, especially in comparison with those of the Cloisite 93A membrane (retention = 85%, flux = 14.8 L/m^2 h).

Generally, membrane performances depend not only on the porosity and thickness of the skin layer but also on the membrane hydrophilicity. The latter property improves the membrane resistance to fouling and, consequently, allows better stability of the permeate flux with the operating time.[23]

The contact-angle measurement between a drop of water and a flat smooth surface is commonly considered to be a very simple and convenient method for evaluating surface wetting.[24] Therefore, this measurement can be used to obtain qualitative information on the membrane hydrophilicity.

In this work, dense films were used for contact-angle measurements to avoid any possible effect due to the membrane porosity.

The results listed in Table IV show that only Cloisite 30B is capable of modifying the contact angle, and the more Cloisite 30B clay is added to the casting solution, the lower the contact angle is. The main reason that the two other types of clays do not affect the contact angle is their poor dispersion in the composite films.

The mechanical properties of the prepared films are given in Table V.

In comparison with the neat PSU film, an increase in Young's modulus can be observed for all the composite films. The tensile modulus increases with increasing clay concentration. Comparing films with the same layered-silicate concentration, we should point out that Cloisite 30B, which is the best dispersed system, gives the highest modulus, especially at a low clay concentration (2 wt %). This result was expected because clay particles inherently possess high moduli and, if dispersed at the nanoscale level, should also increase the moduli of polymer systems. However, the tensile modulus of PSU/Cloisite Na turns out to be comparable to that of PSU/Cloisite 30B when the clay concentration is increased (3 wt %). This phenomenon is likely due to the layered-silicate aggregation, which prevents the formation of nanostructured systems characterized by a high factor form.

On the contrary, the tensile strength and the strain at break decrease with the addition of clay. The same phenomenon has been observed for other polymer/clay systems.[25]

CONCLUSIONS

Novel porous membranes and dense films composed of clay particles homogeneously dispersed in a porous PSU structure have been developed.

SEM, TEM, and X-ray diffraction measurements have proved that, among the different types of clay used, only Cloisite 30B is dispersed at a nanoscopic

TABLE V
Mechanical Properties of the PSU/Cloisite Films

Film type	Clay concentration (wt %)	Strength (MPa)	Tensile modulus (MPa)	Strain at break (%)
PSU	—	77.8	2438	4.9
PSU/Cloisite Na	1	59.5	2633	3.3
PSU/Cloisite Na	2	52.6	2913	2.6
PSU/Cloisite Na	3	48.2	3237	2.4
PSU/Cloisite 30B	2	46.2	3009	3.3
PSU/Cloisite 30B	3	44.1	3289	2.6
PSU/Cloisite 93A	2	48.4	2851	3.5

level. Moreover, this layered silicate has a specific effect on the mechanism of membrane formation.

The incorporation of clay into the membrane structure deeply affects the flux and retention properties. Indeed, nanocomposite films based on Cloisite 30B presented a lower contact angle than those made of neat PSU. This finding highlights the capability of this clay to increase film (or membrane) wettability. Moreover, an improvement in the composite film mechanical properties has been observed. Once again, films based on Cloisite 30B gave the highest moduli.

The precious help of Mauro Michetti and Claudio Uliana with scanning and transmission electron microscopy measurements is gratefully acknowledged. The authors also acknowledge the support of the Nanofun Poly-Network of Excellence (NoE) project ''Nanofun-Poly'' for the diffusion of the research results.

References

1. Zimmerman, C. M.; Singh, A.; Koros, W. J. J Membr Sci 1997, 137, 145.
2. Boom, J. P.; Pünt, I. J. M.; Zwijnenberg, H.; de Boer, R.; Bargeman, D.; Smolders, C. A.; Strathmann, H. J Membr Sci 1998, 138, 237.
3. Genne, I.; Doyen, W.; Adriansens, W.; Leysen, R. Filtr Sep 1997, 34, 964.
4. Bottino, A.; Capannelli, G.; D'Asti, V.; Piaggio, P. Sep Purif Technol 2001, 22, 269.
5. Vankelecom, I. F. J.; DeBeukelaer, S.; Uytterhoeven, J. B. J Phys Chem B 1997, 101, 5186.
6. Cornelius, C. J.; Marand, E. J Membr Sci 2002, 202, 97.
7. Aets, P.; van Hoof, E.; Leysen, R.; Vankelecom, I. F. J.; Jacobs, P. A. J Membr Sci 2000, 176, 63.
8. Merkel, T. C.; Freeman, B. D.; Spontak, R. J.; He, Z.; Pinnau, I.; Meakin, P.; Hill, A. J Chem Mater 2003, 15, 109.
9. Ray, S. S.; Okamoto, M. Prog Polym Sci 2003, 28, 1539.
10. Xu, R.; Manias, E.; Snyder, A. J.; Runt, J. Macromolecules 2001, 34, 1989.
11. Bhardwaj, R. K. Macromolecules 2001, 34, 1989.
12. Messersmith, P. B.; Giannellis, E. P. J Polym Sci Part A: Polym Chem 1995, 33, 1047.
13. Yano, K.; Usuki, A.; Okada, A. J Polym Sci Part A: Polym Chem 1997, 35, 2289.
14. Jung, D. H.; Cho, S. Y.; Peck, D. H.; Skin, D. R.; Kim, J. S. J Power Sources 2003, 118, 205.
15. Alberti, G.; Casciola, M.; Palombari, R. J Membr Sci 2000, 172, 233.
16. Cheng, L.-P.; Lin, D.-J.; Yang, K.-C. J Membr Sci 2000, 172, 157.
17. Bottino, A.; Capannelli, G.; Imperato, A.; Munari, S. J Membr Sci 1984, 21, 247.
18. Dubois, M.; Gilles, K. A.; Hamilton, J. K.; Rebers, P. A.; Smith, F. Anal Chem 1956, 28, 350.
19. Shen, Z.; Simon, G. P.; Cheng, Y.-B. Polymer 2002, 43, 4251.
20. Burgentzlé, D.; Duchet, J.; Gérard, J. F.; Jupin, A.; Fillon, B. J Colloid Interface Sci 2004, 278, 26.
21. Aets, P.; Genne, I.; Kuypers, S.; Leysen, R.; Vankelekom, I. F. J.; Jacobs, P. A. J Membr Sci 2000, 178, 1.
22. Parvulescu, V.; Buhoci, L.; Roman, G.; Albu, B.; Popescu, G. Sep Purif Technol 2001, 25, 25.
23. Möckel, D.; Staude, E.; Guiver, M. D. J Membr Sci 1999, 158, 63.
24. Neumann, A. W.; Good, R. J.; Hope, C. J.; Sejpal, M. J Colloid Interface Sci 1974, 49, 291.
25. Delozier, D. M.; Orwoll, R. A.; Cahoon, J. F.; Johnston, N. J.; Smith, J. G., Jr.; Connell, J. W. Polymer 2002, 43, 813.